

Monitoring the chemical changes in fingerprint residue over time using synchrotron infrared spectroscopy

Rhiannon E Boseley,¹ Jitraporn Vongsvivut,² Dominique Appadoo,² Mark J Hackett^{1*} & Simon W Lewis^{1*}

¹School of Molecular and Life Sciences, Curtin University, GPO Box U1987, Perth, Western Australia 6845, Australia

²ANSTO – Australian Synchrotron, 800 Blackburn Road, Clayton, Victoria 3168, Australia



Abstract

Degradation of fingerprint residue has a major impact on the successful forensic detection of latent fingerprints. The time course of degradation has been previously explored with bulk chemical analyses, but little is known about chemical alterations at the micron-scale. Here we report the use of synchrotron-sourced attenuated total reflection-Fourier transform infrared (ATR-FTIR) microscopy to provide spatio-temporal resolution of chemical changes within fingerprint droplets, as a function of time since deposition. Eccrine and sebaceous material within natural fingerprint droplets were imaged on the micron scales at hourly intervals for the first 6 – 12 hours after deposition, revealing that substantial dehydration occurred within the first 8 hours. Changes to lipid material was more varied, with samples exhibiting an increase or decrease in lipid concentration due to the degradation and redistribution of this material. Across 12 donors, it was noticeable that the initial chemical composition and morphology of the droplet varied greatly, which appeared to influence on the rate of change of the droplet over time. Further, this study attempted to quantify the total water content within fingerprint samples. The wide-spread nature and strength of the absorption of Terahertz/Far-infrared (THz/Far-IR) radiation by water vapour molecules were exploited for this purpose, using THz/Far-IR spectroscopy. Upon heating, water confined in natural fingerprints was evaporated and expanded in a vacuum chamber equipped with multipass optics. The amount of water vapour was then quantified by high-spectral resolution analysis, and fingerprints were observed to lose approximately 14 – 20 μg of water. The combination of both ATR-FTIR and Far-IR highlight important implications for experimental design in fingerprint research, and operational practices used by law enforcement agencies.

Introduction

Fingerprint ridge patterns are characteristic to an individual, with the marks left following contact between the fingertip and a surface frequently utilised for identification purposes in forensic science.¹ The residue left on contact is often invisible to the naked eye, requiring chemical or physical treatment to enable detection. Despite ongoing research to improve fingerprint visualisation procedures, there remains significant detection challenges due to the chemical variability of a fingerprint.² Following deposition there are changes in morphology and the chemistry of fingerprint residue due to interaction with the surface, the sample environment, and the fingerprint residue itself.³ The above factors can impact fingerprint chemistry at variable rates, hindering successful fingerprint development.³ Whilst the surface and sample environment are conditions which can be controlled and monitored, the chemistry of fingerprint residue is multifaceted and more variable and therefore, is an area of interest for fingerprint researchers.

Fingerprint residue is made primarily of a mixture of secretions from the eccrine and sebaceous glands, and is likely to be contaminated with constituents picked up through contact during daily activity.⁴⁻⁶ Once deposited, this residue is not static with a potential to move across a surface, and undergo chemical and physical changes. Sebaceous material is an oily mixture of lipids, which are known to degrade over time, studies have attempted to correlate this rate of degradation to time since fingerprint deposition.⁷⁻⁹ However, as the lipids may originate from different sources, such as sebaceous glands or from physical contact with certain parts of the body, there can be large variation in the initial lipid content and composition, which makes age prediction of fingerprints challenging.^{10, 11} The eccrine substituents are an aqueous mixture containing amino acids, salts and proteins. The water content undergoes evaporation as one of the first signs of degradation, which can be a main driver towards altering the physical and chemical properties of the remaining residue.^{12, 13}

The water content of fingerprints is known to decrease as a function of time since deposition, yet, fundamental knowledge, such as the exact amount of water contained in a fingerprint is not well known. The water content is known to have a direct impact on fingerprint detection, with dried, aged fingerprints showing weaker performance when detected with some operational methods.¹⁴⁻¹⁷ There are inherent challenges when attempting to measure the quantities of material present within a fingerprint due to the small quantities and variability of material present. The water fraction of a fingerprint is expected to make up a significant portion by mass; however, there have been many conflicting reports on how much water is within a fingerprint and its rate of evaporation.^{12, 18, 19} Current methods have used microbalances to measure the mass of this material and its change over time with great disparity in the findings.^{12, 18} Keisar *et al.* calculated the mass of a fingerprint to be between 2 –

9 μg , based on the weight of a smaller subsection of the mark, whilst Bleay *et al.* reported a mass range of 0.33 – 29 μg .^{6, 18}

Several studies have explored fingerprint degradation, by visually comparing how fingerprint development methods are affected by evaporation and time since deposition.^{14, 17, 20, 21} An alternative approach has been to explore the chemical alteration within fingerprint residue, by directly measuring the chemical constituents present at different time points since deposition, using techniques such as gas chromatography (GC) and liquid chromatography – mass spectroscopy (LC-MS).^{7-10, 22-24} Whilst each of these methods can provide valuable bulk chemical information on the degradation process, spatially resolved chemical information is not provided. A method or methods, which can determine both chemical specificity and spatial information can provide a better overall picture of fingerprint residue as it ages.²⁵

Recent advances in scientific capabilities have utilised methods such as atomic force microscopy (AFM), x-ray fluorescence microscopy (XFM) and attenuated total reflection-Fourier transform infrared (ATR-FTIR) microscopy, to bring together spatial and chemical specific information on fingerprint residue.²⁶⁻²⁸ There are a number of advantages to these methods, particularly the capability to image fingerprints without any chemical alteration, treatments, or solvent extractions prior to measurement. In-situ label-free measurements, where possible, can give a more realistic representation of the chemical species naturally present in fingerprint residue. The spatial resolution of these techniques is on the micron scale, and therefore allows investigation of individual droplets in fingerprint residue. As an example, synchrotron-sourced ATR-FTIR microspectroscopy was recently used to identify the distribution of eccrine and sebaceous components present within a single droplet.²⁸ The application of these methods provides the opportunity to further understand the degradation of fingerprint residue, by directly imaging the chemical and morphological changes of the eccrine and sebaceous material within a natural fingerprint as a function of time since deposition.

In this study, we exploit the unique characteristic of the highly intense synchrotron-IR beam that allows shorter data collection time, while still maintaining high spectral quality, and the advantage of enhanced spatial resolution (down to 2-3 μm) offered by the synchrotron ATR-FTIR microspectroscopic technique, to measure the chemical changes within a fingerprint droplet as a function of time since deposition.²⁹ Further, the Terahertz/Far-infrared (THz/Far-IR) region offers sensitivity to pure-rotational water vapour transitions and provides an intriguing opportunity to measure the total water content in fingerprint residues by heating the sample and evaporating the water into the gas phase for high spectral resolution analysis. Taken together, the results from synchrotron-sourced ATR-FTIR microspectroscopy and THz/Far-IR spectroscopy in the gas phase

provide new insights into the chemical changes that occurred within fingermarks as a function of time since deposition, as well as an estimate of the total initial water content contained within a fingermark.

Experimental

Synchrotron ATR-FTIR Microspectroscopy

Fingermark Deposition

Fingermarks were deposited directly onto the ATR germanium (Ge) hemispherical crystal by lightly pressing the centre of the fingertip on the centre of the crystal for 5 seconds (See Figure 1C). Natural fingermarks were collected from 12 donors, donor information is provided in Table 1.

Table 1: Fingermark Donor Information

Donor	Age	Gender	Cosmetic Use
1	78	Male	None reported
2	27	Female	None reported
3	22	Male	None reported
4	24	Male	None reported
5	41	Male	None reported
6	24	Female	Yes
7	55	Male	Yes
8	48	Male	None reported
9	26	Female	Yes
10	41	Female	Yes
11	-	Female	None reported
12	23	Female	None reported

Instrumentation and Data Collection

Synchrotron ATR-FTIR experiments were conducted on the Infrared Microspectroscopy (IRM) beamline at the ANSTO – Australian Synchrotron (Clayton, Victoria). The FTIR instrument on the IRM beamline consists of a Bruker Hyperion3000 microscope coupled to a Bruker Vertex V80v FTIR spectrometer, with a liquid nitrogen cooled mercury cadmium telluride (MCT) narrow band detector (Bruker Optik GmbH, Ettlingen, Germany). The ATR-FTIR accessory was equipped with a germanium (Ge) hemispherical crystal ($n_{\text{Ge}} = 4.0$), which has a 1 mm diameter active sensing area. Spectral maps were acquired using a 20× objective (NA = 0.60; Bruker Optik GmbH, Ettlingen, Germany), with an effective spot size of 1.88 μm on the sample surface and a step interval of 1 μm between the measurement points. A background spectrum of the clean Ge-ATR crystal was measured using 256 co-added scans and 8- cm^{-1} spectral resolution. Each sample spectrum was recorded using 4 co-added scans and 8- cm^{-1} spectral resolution. The experiment was performed under ambient room conditions without nitrogen purge and with opened purge box, to ensure a natural evaporation of water in the fingermarks throughout the measurement. Data acquisition and analysis were conducted using OPUS v8.0 software suite (Bruker).

Data Analysis

The raw FTIR spectral maps were first pre-processed for the ATR correction to take account of the refractive index of the Ge ATR crystal, and atmospheric compensation before further analysis using the OPUS v8.0 (Bruker) and CytoSpec 2.00.03 software (Cytospec Inc., Boston, MA, USA). The ATR-FTIR chemical images were further processed with ImageJ 1.50i software.

Synchrotron THz/Far-IR Spectroscopy

Sample Preparation

In order to study the water content in fingermarks, a standard 200 mm long 5 mm in diameter chemistry glass rod was used to deposit the fingermarks of donors 7 and 10 (see Table 1 for donor information). The glass rod was first cleaned with isopropanol and left to warm to room temperature prior to sample deposition. Then, the fingermarks were deposited by rolling the fingertips across a glass rod back and forth for 5 seconds. Three types of fingermarks were collected, and are outlined in Table 2; these types were decided based on the varying amounts of water that could be yielded.

Table 2: THz/Far-IR Fingermark Sample Types

Sample Type	Sample Preparation
Natural	Donor was instructed to go about their daily activities for 30 minutes, no washing of the hands in this time.
Air	Donor was instructed not to touch anything for 30 minutes, hands were open to atmosphere
Gloves	Donor was instructed not to touch anything for 20 minutes then wore nitrile gloves for 10 minutes

In order to quantify the amount of water detected in the donor fingermarks, a calibration curve was generated from carefully measured volumes of deionised water (0.25 μL , 0.5 μL , 0.875 μL , 1.25 μL , and 1.5 μL). The water was deposited in the middle of the glass rod using a 0.1 – 2.5 μL pipette.

Instrumentation

In this study, we used a furnace to heat a 300 mm long Qz tube with a 20 mm inner diameter coupled to 10 L glass gas-cell via the gas-manifold located on a mobile gas-handling vacuum (MGHV) system. The gas-cell itself was placed on the sample compartment of a Bruker IFS125/HR FT spectrometer. The quartz tube was heated to 70 (+/-0.5) $^{\circ}\text{C}$ using the furnace while the gas cell was heated to 70 (+/-5) $^{\circ}\text{C}$ using heating tapes.

For these measurements, the optical configuration of the spectrometer consisted of a 12.5 mm aperture, a 6 μm multilayer Mylar beamsplitter, and a 4.2 K Si bolometer from Infrared Laboratories equipped with a PE window and a 13 μm thick stretched PE film cold filter ($< 800\text{ cm}^{-1}$). The spectra were recorded at 0.01 cm^{-1} spectral resolution, at a scanner speed of 2.5316 cm/s (40 kHz),

and the pre-amplifier gain on the Si bolometer was set to 200. Sets of 10 scans were accumulated yielding a signal-to-noise (S/N) ratio of approximately 194.

The gas-cell is made of borosilicate glass, and with variable path-length gold-coated optics, M35V, from Infrared Analysis; the cell has a nominal single path-length of 625 mm, and the number of times the light can be bounced off its mirrors can be varied from 4 up to 56 times in multiples of 4, yielding an optical path-length from 2.5 m to 35 m. For this spectral region, the gas-cell was equipped PE wedged windows, and the path-length set to 2.5 m.

Data Collection

The complete system consisting of the furnace, MGHV system and gas-cell was first evacuated to its base pressure ($< 1 \times 10^{-3}$ mbar). Prior to inserting a sample, the furnace was isolated from the vacuum and was brought up to atmospheric pressure and purged with dry $N_2(g)$ from the pressurised boil-off of the $N_2(l)$ tanks. The flow of the purged $N_2(g)$ was halted during sample insertion to prevent any H_2O in the fingerprints from being sublimed; then, the furnace was sealed and isolated after sample insertion while the sample line was evacuated to base-pressure. After the system (excluding the furnace) was brought back to base pressure, a measured amount (~ 5 mbar) of the warm gas mixture consisting of $H_2O(g)$ mainly from the rod, fingerprints and the purged $N_2(g)$ was allowed to flow from the furnace into the gas cell for analysis.

Data Analysis

All raw FTIR spectra were measured and analysed using Bruker OPUS v8.0. A background spectrum was first recorded, and was used to calculate the absorbance spectrum of each sample. For the background spectra, a cleaned glass rod was inserted in the quartz tube, and the warm gas mixture consisting mainly of $H_2O(g)$ from the rod and the dry $N_2(g)$ was allowed to flow from the furnace into the gas cell for analysis the gas-cell was filled with 5.01 mbar of $N_2(g)$.

The absorbance spectrum of each sample was first normalised to the pressure when the background spectrum was recorded (5.01 mbar) before the background absorbance was subtracted from the sample absorbance to yield the true absorbance of H_2O coming from the fingerprint samples only (sample = H_2O droplets and fingerprints).

Results and Discussion

Study 1 – The chemical and morphological changes in eccrine and lipid material within natural latent fingerprints in the first 12 hours following deposition.

In this study, the chemical and morphological changes of individual droplets within natural fingerprints were measured in the first 6 - 12 hours following sample deposition using synchrotron ATR-FTIR technique. Specifically, spectroscopic marker bands of eccrine and sebaceous material were monitored (eccrine marker: O-H stretching ($3000\text{-}3500\text{ cm}^{-1}$), sebaceous marker: C-H stretching of lipids ($2800\text{-}3000\text{ cm}^{-1}$)), as per our previous studies.^{26, 28}

Twelve donors provided fingerprint samples in which droplets containing eccrine and lipid material could be identified. Across each sample, it was noticeable that the fingerprints deposited by different donors showed diverse morphology and varied composition of lipid and eccrine material, which were consistent with our past work.^{26, 28} Figure 1 shows a representative sample of a fingerprint droplet provided by donor 1. This particular sample appears to be a central eccrine droplet surrounded with lipid material. Across a period of 7 hours, there is a noticeable change in lipid and eccrine concentration, based on the C-H stretching ($2800\text{-}3000\text{ cm}^{-1}$) and O-H stretching ($3000\text{-}3500\text{ cm}^{-1}$) bands, previously reported to be indicative of these substituents.²⁸ This sample shows an exponential decrease in the signal attributed to the eccrine material, based on the average intensity of the O-H stretching peak integrated across the droplet area. This trend can be further observed when looking directly at the spectra extracted from the images (Figure 2), where the peak intensity of the O-H stretching peak ($3000\text{-}3500\text{ cm}^{-1}$), and the O-H bending peak ($1540\text{-}1700\text{ cm}^{-1}$) can be clearly seen to decrease as the time since deposition increases. In contrast, the opposite trend is seen for sebaceous material, with a clear increase in peak intensity for the C-H stretching ($2800\text{-}3000\text{ cm}^{-1}$) band (Figure 2).

A decrease in water content was observed across 10 donors over time, as represented in Figure 3, with the water content appearing to plateau after approximately 8 hours. As eccrine material is an aqueous mixture, the reduction in water content can be attributed to evaporation. This extends on recent work by Keisar *et al.*, which explored the evaporation of water within the first few minutes post fingerprint deposition.¹⁸ Although demonstration that water evaporates from a fingerprint is not particularly surprising, a key observation from these results has been the evidence that water can continue to evaporate from a fingerprint sample at room temperature for at least 8 hours.

In addition, the lipid concentration and distribution were observed to be more varied with greater disparity seen across donors compared to the eccrine material. The sample shown in Figure 1 demonstrates an increase in lipid material, this was consistent with 5 donors, whilst the remaining 7 donors decreased in overall lipid concentration. The discrepancies could be justified by the increase in

concentration of the residual lipid content, and also the redistribution of lipid material that led to an increase in contact areas between the lipid material and the Ge crystal as a result of the water evaporation. Interestingly, a distinct pattern of changes in lipid composition was observed. The C-H stretching peaks ($2800\text{-}3000\text{ cm}^{-1}$) showed a gradual increase over the 8 hour period, suggesting an increase in lipid concentration. However, the C=O stretching region ($1715\text{-}1750\text{ cm}^{-1}$) decreased in the first 4 hours and then increased between 4 to 8 hours. These results could indicate initial degradation of lipid material before the potential oxidation of these compounds.

The oxidation of sebaceous lipids, such as squalene, cholesterol and unsaturated fatty acids, has previously been reported in studies aiming to predict fingermark age.^{7, 21, 30} Factors influencing the starting material in fingermark residue have been shown to have a major impact on the rate of degradation of these components, making it impossible to identify universal trends.^{5, 11} The findings reported here reinforce the challenges of calculating time since deposition, with significant variation appearing within the morphology and lipid composition of single droplets in fresh natural fingermarks. These studies focused on the first 12 hours since deposition, further work should be done to explore a longer time period to investigate whether further morphological and chemical changes can be observed on the macro scale with this method over longer time periods.

Noticeably, Donor 12 was an anomaly with the O-H peak intensity increasing over the first 8 hours (Figure 3). To investigate further, measurements were repeated with this donor by taking triplicate fingermark samples (Figure 4). The two repeat measurements behaved more consistently with the rest of the data for eccrine material, displaying a time-dependent decrease in the O-H peak, which can be ascribed as water content in the eccrine material (Figure 4). We attribute the variation in response from donor 12, to the high lipid content present in the initial fingermark and the large size of the droplet. The droplet imaged in replicate 1 appeared to cover the entire imaged area, meaning the droplet size was $> 80 \times 80\ \mu\text{m}^2$, whereas replicates 2 and 3 were smaller, fitting within a $75 \times 75\ \mu\text{m}^2$ imaged area. It is understood that the morphological size of the original drop would appear to change the rate of evaporation of water within the sample. It is possible evaporation occurred outside the immediate imaged area, and thereby is not considered within our results. Amongst the triplicate samples from the single donor it was apparent that the lipid material also did not behave consistently, with two replicate measurements showing an increase and one a decrease in lipid material. These results did not appear to be related to droplet size or distribution adjacent to eccrine material, although previous work has demonstrated an increase in lipid degradation when fingermarks were stored in an aqueous environment.²³ On a longer time scale, it is possible that the sebaceous material distributed amongst the aqueous material within a fingermark could influence the rate of degradation. This emphasises how unpredictable the rate of change of a fingermark is, even within the same donor,

suggesting it near impossible to use the chemistry of the fingerprint to predict the time of deposition without knowing the initial chemistry of the residue.

This study is the first report to use chemical imaging techniques to demonstrate how fingerprint chemistry changes in the immediate hours following deposition, and has important implications for fingerprint research. Specifically, the International Fingerprint Research Group (IFRG) provides guidelines when conducting fingerprint research and recommends the use of fingerprints, which are left to age for a minimum of 24 hours before development.³¹ The results shown here provide context for why fresh fingerprints should not be used for research into latent fingerprint detection techniques, demonstrating the changes in residue chemistry, specifically the evaporation of water content that can occur within the first 8 hours following deposition. By leaving fingerprints for 24 hours, researchers can provide a more realistic representation of what would be encountered in casework as it is unlikely for fingerprints to be collected within the hours immediately following transfer of material. Whilst this study focused primarily on the first 12 hours following deposition, further work should be conducted to see whether additional changes can be seen in the morphology and chemical composition of the droplet for a longer time frame.

Study 2 – Measuring the volume of water lost through evaporation of latent fingerprints

The results from study 1 demonstrated that eccrine material in a fingerprint showed a substantial change in the first hours since deposition, thus impacting the chemical composition and the morphology of the mark as it ages. Whilst eccrine sweat is made up of 99% water, water is estimated to comprise anywhere between 20-70% of the total fingerprint residue, varying significantly between donors based on a range of factors.^{18, 19} There are a number of challenges in measuring the volume of material deposited in fingerprint residue, with the inherent variability and influence from the surrounding environment, making it difficult to standardise an analytical approach. Recent work has utilised a quartz crystal microbalance (QCM) to determine the amount of water lost through evaporation from a fingerprint sample.^{6, 18} The results demonstrated that the majority of water content was evaporated in the first few minutes following deposition, however the results shown here in study 1 suggest there is a longer time period of evaporation.¹⁸ In study 2, we used high-spectral resolution gas-phase THz/Far-IR spectroscopy to estimate the total volume of water contained in a fingerprint. Fingerprints were heated to 70 degrees, and the water content measured in the gas phase using a gas cell with 2.5 m optical path difference. The water content was determined using a linear calibration, developed from the rotational spectrum of water; a portion of the rotational spectrum void of strong and overlapping peaks was selected, in particular a peak located at 202.69 cm⁻¹ was chosen (see Figure 5). A plot of the absorbance intensities with respect to volume of H₂O deposited on the glass rod showed a linear relationship with an R^2 value of 0.9932. This linear relationship was

then used to predict the volume of water in the fingerprint sample, outlined in Figure 6. Of the three sets of fingerprints taken the natural fingerprints had the lowest water content, between 14-20 μg (volume of water converted to mass of water, assuming a density of 1 g/mL). Two further samples were taken, fingerprints deposited after the hands were left in the air for 30 minutes, minimising contact with a surface and fingerprints deposited after wearing nitrile gloves for 10 minutes. These samples demonstrated increased water content, 60-79 μg and 77-101 μg respectively. The increase in water content could possibly be attributed to the loss of material on the surface of the hands in natural daily behaviour, by minimising contact with a surface the eccrine material is left to build up on the fingertip, potentially increasing the material deposited in this study. Wearing gloves can increase the amount of eccrine material produced by increasing the perspiration rate from the hands, and therefore the increase in water content calculated from these samples is not unexpected.³

The literature contains few reports concerning the determination of the mass of a fingerprint, which are often conflicting with respect to the volume of water present in fingerprint residue.^{6, 12, 18} This is most likely due to the challenge of working on the microscale with material so sensitive to change and influence from the surrounding environment. The measurements recorded in this study are higher than that reported by Keisar *et al.*, with their total fingerprint mass calculated to be between 2 – 9 μg .¹⁸ Their approach measured a 0.2 cm^2 area of the fingerprint ($\sim 1/10^{\text{th}}$ of the full fingerprint surface area) using a QCM, with the entire mass calculated using the Sauerbrey equation, not taking into account the inherent variability across a fingerprint.¹⁸ Bleay *et al.* reports studies which measured a fingerprint mass across a range of 0.33 and 29.00 μg , with large discrepancies not unexpected as the water content is anticipated to vary significantly between samples.⁶ The results shown here for natural fingerprints appear to lie at the upper range of this mass, suggesting the water content could comprise 40 – 70% of the total fingerprint mass – a figure which aligns with recently proposed values in literature.¹⁸ Further work should consider the correlative use of high-spectral resolution gas-phase THz/Far-IR spectroscopy alongside microbalance measurements, using an increased number of donors to improve the accuracy of this method and provide complementary data to assist in the determination of the volume of water lost through evaporation of fingerprint samples.

Conclusions

This study has reinforced the complexity of fingerprint chemistry using synchrotron FTIR spectroscopy in both mid-IR and THz/Far-IR spectral ranges. Single droplets within natural fingerprints from 12 donors were imaged at the micron scales using the synchrotron ATR-FTIR technique. The variation in the initial chemical composition and morphology has demonstrated a significant impact on the rate of change of the droplet over time, highlighting the inherently complex nature of this biological material. Broadly, there is a noticeable change within the fingerprint sample in the immediate hours

following deposition, with a decrease in water content seen within the first 8 hours. The lipid material is more multifaceted, with samples shown to both increase and decrease in lipid concentration following deposition due to the degradation and redistribution of lipid material. The results challenge the suggestion that one can simply predict the age since deposition of a fingerprint. The variability of interdonor and intradonor fingerprint chemistry corroborates the unpredictable nature of the rate of change of fingerprint residue, particularly without knowledge of the initial material present. By imaging this change in the first few hours, we have explicitly shown how dynamic fingerprint residue is, which must be considered in both operational and research contexts.

To determine the extent of change in water content, high-spectral resolution gas-phase THz/Far-IR spectroscopy was used to quantify the amount of water that could be evaporated from a fingerprint sample. The intensity of the rotational transitions of water vapour were measured to determine the approximate loss of water ranging between 14 to 101 μg for natural fingerprints and those which had been groomed for increased water content. The results appear to be within the same range as those recently reported for natural fingerprints;⁶ however, given the highly variable nature of fingerprint material further work should be conducted with a wider range of donors to provide a more developed understanding of the potential of this method to measure water within fingerprint residue.

Acknowledgements

Components of this research were undertaken at the Infrared Microspectroscopy and the THz/Far-IR Spectroscopy beamlines, at the Australian Synchrotron, part of ANSTO (Victoria, Australia). The authors acknowledge the contribution of an Australian Government Research Training Program Scholarship and Australian Institute of Nuclear Science and Engineering Postgraduate Research Award (REB) in supporting this research. The authors thank all the fingerprint donors for their co-operation, Wilhelm van Bronswijk for his guidance throughout this study, and to those who contributed their time to assist in data collection. This project has been approved by the Curtin University Human Research Ethics Committee (Approval Number HRE2018-0476).

Author Contributions

Rhiannon E. Boseley: Conceptualization; methodology; investigation; formal analysis; visualization; writing - original draft; writing - review and editing. **Jitraporn Vongsvivut:** Conceptualization; methodology; investigation; supervision; writing - review and editing. **Dominique Appadoo:** Conceptualization; methodology; investigation; writing - review and editing. **Mark J. Hackett:** Conceptualization; supervision; writing - review and editing. **Simon W. Lewis:** Conceptualization; project administration; supervision; writing - review and editing

Figures

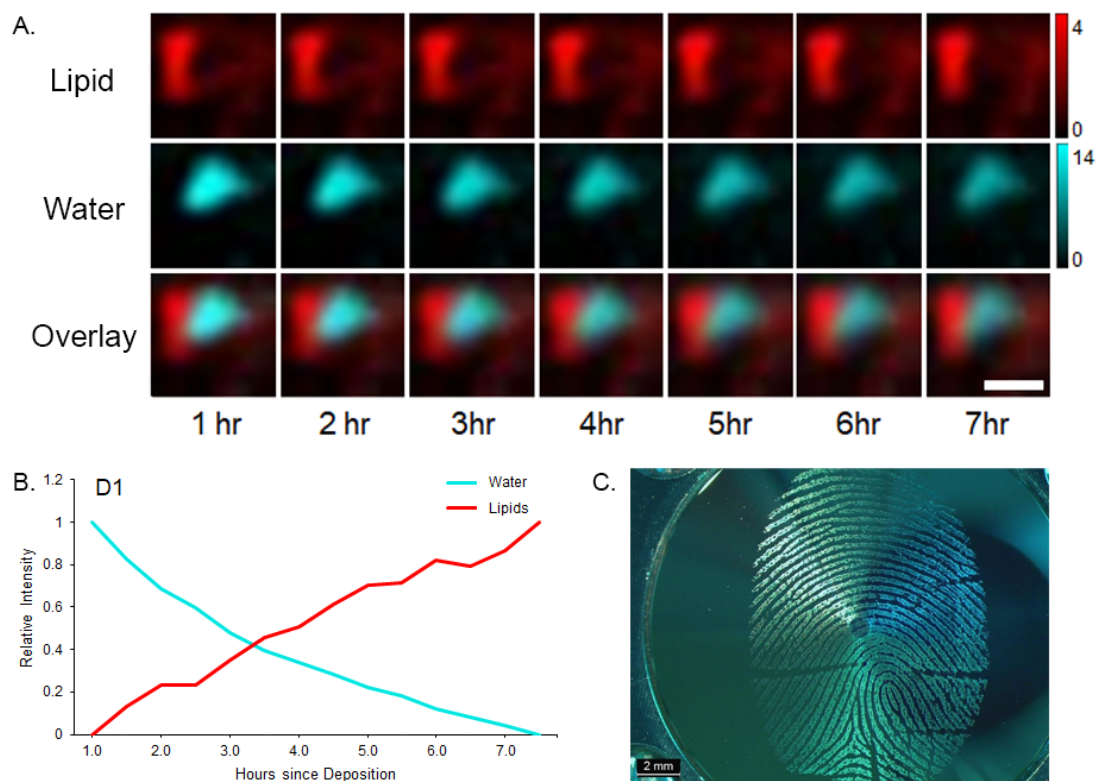


Figure 1: (A) Representative example of time-course (7 hour) changes in lipid and H₂O content during air-drying of a natural fingerprint, as revealed by ATR-FTIR mapping approach. False colour ATR-FTIR maps were generated by integrating over the $\nu(\text{C-H})$ stretching bands (2800-3000 cm^{-1}) as a marker of lipid material (top row) and $\nu(\text{O-H})$ stretching bands of H₂O (3000-3500 cm^{-1}) as a marker for eccrine material (middle row). Overlay images are displayed in the bottom row. Scale bar 20 μm . (B) The relative changes in lipid and H₂O content as a function of air-drying time can also be visualised as the normalised average band area calculated across the entire droplet. Representative sample corresponds to Donor 1 (D1). (C) representative optical image of a natural fingerprint deposited on the Ge ATR crystal for the analyses undertaken in this study.

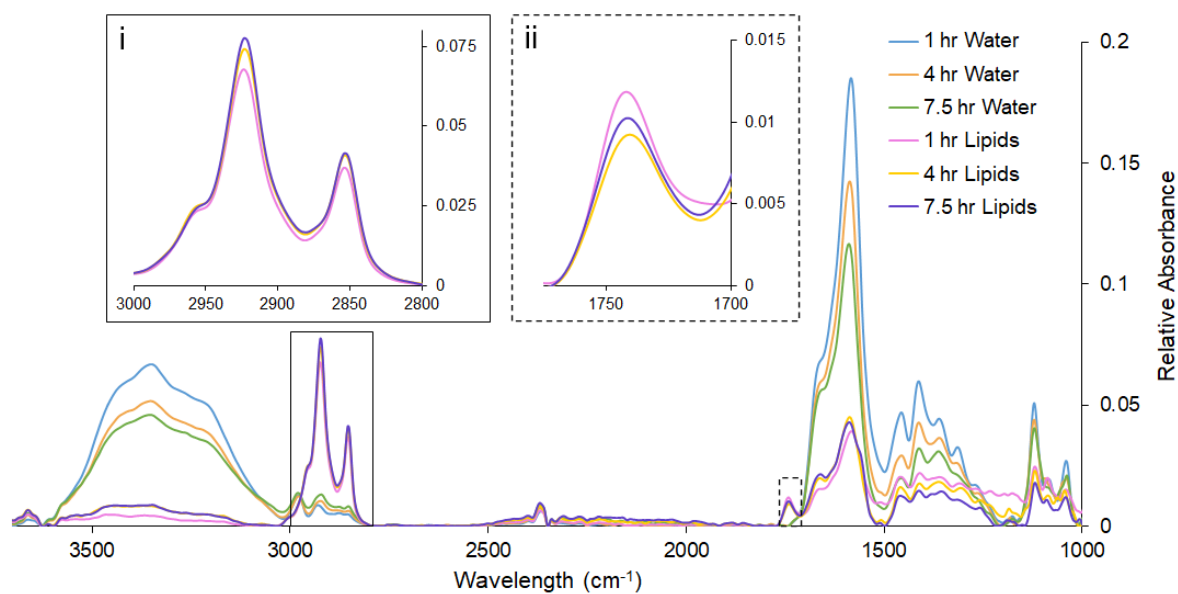


Figure 2: Representative examples of ATR-FTIR spectra collected from a natural fingerprint after 1 hour, 4 hours, and 7.5 hours of air-drying period (from the same dataset presented in Figure 1, donor 1). Representative spectra are presented from image regions enriched in lipid material or water (using H₂O content as a marker of eccrine components). The most pronounced changes in lipid concentration are highlighted in (i) v(C-H) stretching band (2800-3000 cm⁻¹) and (ii) v(C=O) stretching band (1715-1750 cm⁻¹).



Figure 3: Time-dependent changes in H₂O content (as a marker of eccrine material) and lipid content during air-drying of natural fingermarks was measured for 12 individual fingermarks (donors 1 – 12), using the same ATR-FTIR approach. As expected, a strong time-dependent decrease in H₂O content was observed in donors 1-10 (cyan), with exceptions observed in donors 11 and 12. The H₂O content was measured as the integrated area across $\nu(\text{O-H})$ absorbance bands (3000 – 3500 cm⁻¹), and lipid content (red) was measured across $\nu(\text{C-H})$ absorbance bands (2800 – 3000 cm⁻¹). The average band area was calculated across the entire fingermark droplet.

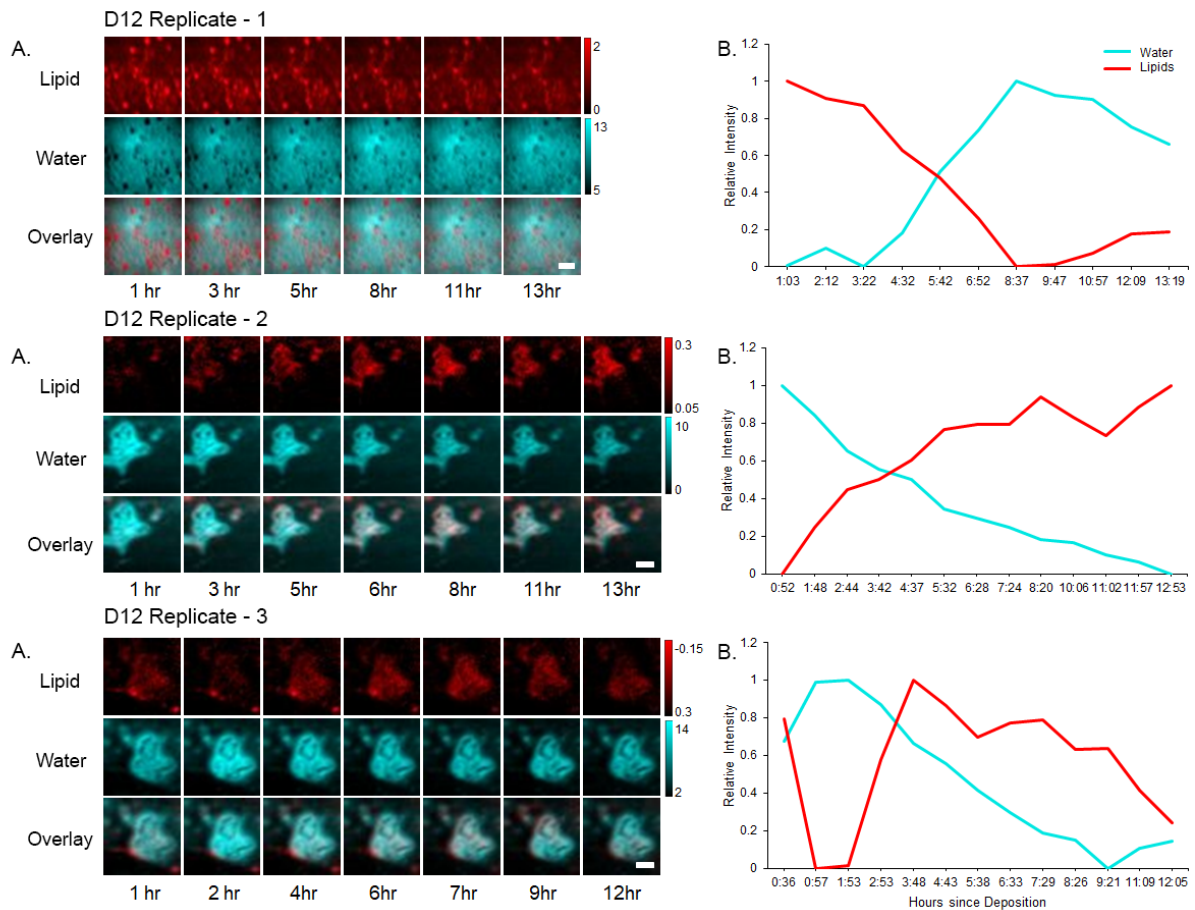


Figure 4: Analysis of intra-donor variance in triplicate fingermarks from donor 12. **(A)** False colour ATR-FTIR maps were generated by integrating over the $\nu(\text{C-H})$ stretching bands ($2800\text{-}3000\text{ cm}^{-1}$) as a marker of lipid material (top row) and $\nu(\text{O-H})$ stretching bands of H_2O ($3000\text{-}3500\text{ cm}^{-1}$) as a marker for eccrine material (middle row). Overlay images are displayed in the bottom row. **(B)** The relative changes in lipid and H_2O contents as a function of air-drying time can also be visualised as the normalised average band area calculated across the entire droplet. Scale bar $20\text{ }\mu\text{m}$.

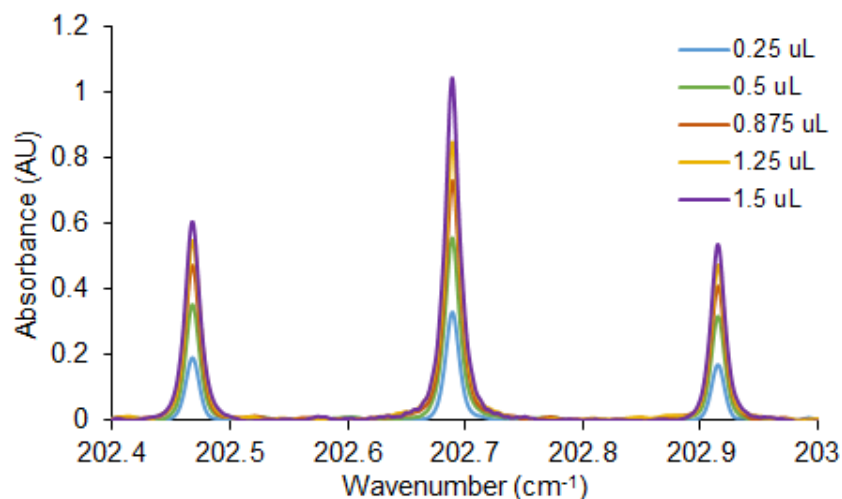


Figure 5: THz/Far-IR gas phase spectra showing H₂O pure-rotational spectral lines for calibration samples, highlighting the linear response between band intensity and volume of water from which the gas phase sample was generated (0.25 μ L, 0.5 μ L, 0.875 μ L, 1.25 μ L, and 1.5 μ L). The selected spectral region shows the rotational transitions of H₂O at 202.47 cm^{-1} , 202.69 cm^{-1} and 202.92 cm^{-1} .

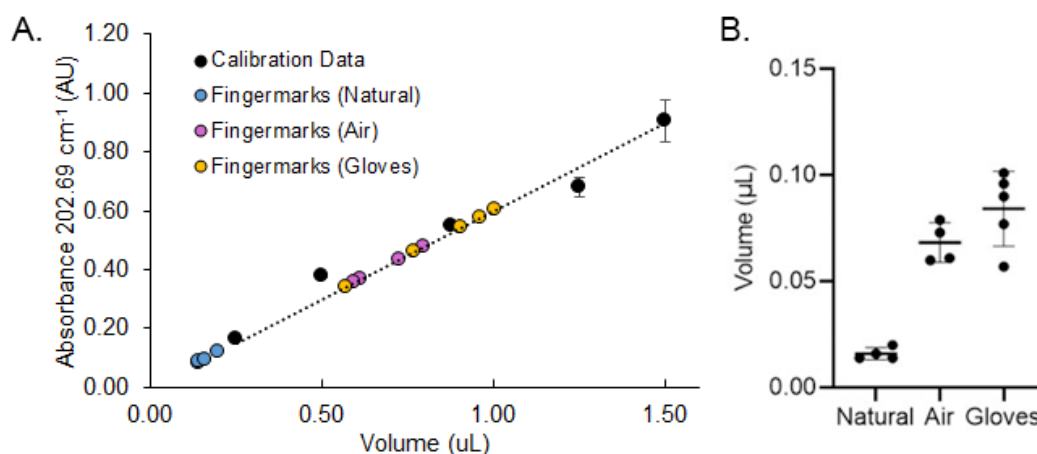


Figure 6: (A) The volume of water contained in a latent fingerprint was quantified from the calibration curve (black dots, $R^2 = 0.9932$) using the rovibrational transition of H₂O at 202.69 cm^{-1} . (B) The volume of water was calculated for natural fingerprints ($n = 4$), fingerprints with hands left in the air for 30 minutes ($n = 4$), and fingerprints after wearing gloves for 10 minutes ($n = 5$). Volume shown for each data point in panel A, is for a set of 10 fingerprints deposited onto a sample substrate. The volume of water for each sample was therefore, divided by 10, to give an average water volume per fingerprint (as shown in panel B). Error bars in A, and B are equal to 2σ .

References

1. Barnes, J. G., Chapter 1: History. In *The fingerprint sourcebook*, National Insistute of Justice: 2011.
2. Chadwick, S.; Moret, S.; Jayashanka, N.; Lennard, C.; Spindler, X.; Roux, C., Investigation of some of the factors influencing fingermark detection. *Forensic Science International* **2018**, *289*, 381-389.
3. Sears, V. G.; Bleay, S. M.; Bandey, H. L.; Bowman, V. J., A methodology for fingermark research. *Science & Justice* **2012**, *52* (3), 145-160.
4. Frick, A. A.; Fritz, P.; Lewis, S. W., Chemistry of Print Residue In *Encyclopedia of Forensic Sciences*, Saukko, P. J.; Houck, M. M., Eds. Academic Press: Waltham, 2013; pp 92-97.
5. Girod, A.; Ramotowski, R.; Weyermann, C., Composition of fingermark residue: A qualitative and quantitative review. *Forensic Science International* **2012**, *223* (1), 10-24.
6. Bleay, S. M.; Bailey, M. J.; Croxton, R. S.; Francese, S., The forensic exploitation of fingermark chemistry: A review. *WIREs Forensic Science* **2021**, *3* (4), e1403.
7. Mountfort, K. A.; Bronstein, H.; Archer, N.; Jickells, S. M., Identification of Oxidation Products of Squalene in Solution and in Latent Fingerprints by ESI-MS and LC/APCI-MS. *Analytical Chemistry* **2007**, *79* (7), 2650-2657.
8. Archer, N. E.; Charles, Y.; Elliott, J. A.; Jickells, S., Changes in the lipid composition of latent fingerprint residue with time after deposition on a surface. *Forensic Science International* **2005**, *154* (2), 224-239.
9. Pleik, S.; Spengler, B.; Ram Bhandari, D.; Luhn, S.; Schäfer, T.; Urbach, D.; Kirsch, D., Ambient-air ozonolysis of triglycerides in aged fingerprint residues. *Analyst* **2018**, *143* (5), 1197-1209.
10. Cadd, S.; Islam, M.; Manson, P.; Bleay, S., Fingerprint composition and aging: A literature review. *Science & Justice* **2015**, *55* (4), 219-238.
11. Frick, A. A.; Girod-Frais, A.; Moraleda, A.; Weyermann, C., Latent Fingermark Aging: Chemical Degradation Over Time. In *De Alcaraz-Fossoul J. (eds) Technologies for Fingermark Age Estimations: A Step Forward*, Springer, Cham.: 2021.
12. Bright, N. J.; Willson, T. R.; Driscoll, D. J.; Reddy, S. M.; Webb, R. P.; Bleay, S.; Ward, N. I.; Kirkby, K. J.; Bailey, M. J., Chemical changes exhibited by latent fingerprints after exposure to vacuum conditions. *Forensic Science International* **2013**, *230* (1), 81-86.
13. Scruton, B.; Robins, B. W.; Blott, B. H., The deposition of fingerprint films. *Journal of Physics D: Applied Physics* **1975**, *8* (6), 714-723.
14. Home Office Centre for Applied Science and Technology *Fingerprint source book v2.0*; UK Government: 2017.

15. Wargacki, S. P.; Lewis, L. A.; Dadmun, M. D., Enhancing the Quality of Aged Latent Fingerprints Developed by Superglue Fuming: Loss and Replenishment of Initiator. *Journal of Forensic Sciences* **2008**, *53* (5), 1138-1144.
16. Sodhi, G. S.; Kaur, J., Powder method for detecting latent fingerprints: a review. *Forensic Science International* **2001**, *120* (3), 172-176.
17. De Alcaraz-Fossoul, J.; Mestres Patris, C.; Balaciart Muntaner, A.; Barrot Feixat, C.; Gené Badia, M., Determination of latent fingerprint degradation patterns--a real fieldwork study. *International Journal of Legal Medicine* **2013**, *127* (4), 857-70.
18. Keisar, O.; Cohen, Y.; Finkelstein, Y.; Kostiry, N.; Ben-David, R.; Danon, A.; Porat, Z. e.; Almog, J., Measuring the water content in freshly-deposited fingermarks. *Forensic Science International* **2019**, *294*, 204-210.
19. Kent, T., Water content of latent fingerprints – Dispelling the myth. *Forensic Science International* **2016**, *266*, 134-138.
20. Jones, N.; Mansour, D.; Stoilovic, M.; Lennard, C.; Roux, C., The influence of polymer type, print donor and age on the quality of fingerprints developed on plastic substrates using vacuum metal deposition. *Forensic Science International* **2001**, *124* (2), 167-177.
21. Mong, G.; Petersen, C.; Clauss, T. *Advanced fingerprint analysis project fingerprint constituents*; Pacific Northwest National Lab., Richland, WA, US, 1999.
22. Frick, A. A.; Chidlow, G.; Goodpaster, J. V.; Lewis, S. W.; van Bronswijk, W., Monitoring compositional changes of the lipid fraction of fingerprint residues deposited on paper during storage. *Forensic Chemistry* **2016**, *2*, 29-36.
23. Dorakumbura, B. N.; Busetti, F.; Lewis, S. W., Analysis of squalene and its transformation by-products in latent fingermarks by ultrahigh-performance liquid chromatography-high resolution accurate mass Orbitrap™ mass spectrometry. *Forensic Chemistry* **2020**, *17*, 100193.
24. Weyermann, C.; Roux, C.; Champod, C., Initial Results on the Composition of Fingerprints and its Evolution as a Function^[11]_{SEP}Of Time by GC/MS Analysis. *Journal of Forensic Sciences* **2011**, *56* (1), 102-108.
25. Hinners, P.; Thomas, M.; Lee, Y. J., Determining Fingerprint Age with Mass Spectrometry Imaging via Ozonolysis of Triacylglycerols. *Analytical Chemistry* **2020**, *92* (4), 3125-3132.
26. Boseley, R. E.; Dorakumbura, B. N.; Howard, D. L.; de Jonge, M. D.; Tobin, M. J.; Vongsivut, J.; Ho, T. T. M.; van Bronswijk, W.; Hackett, M. J.; Lewis, S. W., Revealing the elemental distribution within latent fingermarks using synchrotron sourced x-ray fluorescence microscopy. *Analytical Chemistry* **2019**, *91* (16), 10622-10630.

27. Dorakumbura, B. N.; Becker, T.; Lewis, S. W., Nanomechanical mapping of latent fingerprints: A preliminary investigation into the changes in surface interactions and topography over time. *Forensic Science International* **2016**, *267*, 16-24.
28. Dorakumbura, B. N.; Boseley, R. E.; Becker, T.; Martin, D. E.; Richter, A.; Tobin, M. J.; van Bronswijk, W.; Vongsvivut, J.; Hackett, M. J.; Lewis, S. W., Revealing the spatial distribution of chemical species within latent fingerprints using vibrational spectroscopy. *Analyst* **2018**, *143* (17), 4027-4039.
29. Vongsvivut, J.; Pérez-Guaita, D.; Wood, B. R.; Heraud, P.; Khambatta, K.; Hartnell, D.; Hackett, M. J.; Tobin, M. J., Synchrotron macro ATR-FTIR microspectroscopy for high-resolution chemical mapping of single cells. *Analyst* **2019**, *144* (10), 3226-3238.
30. Pleik, S.; Spengler, B.; Schäfer, T.; Urbach, D.; Luhn, S.; Kirsch, D., Fatty Acid Structure and Degradation Analysis in Fingerprint Residues. *Journal of The American Society for Mass Spectrometry* **2016**, *27* (9), 1565-1574.
31. International Fingerprint Research Group. Guidelines for the Assessment of Fingerprint Detection Techniques. *Journal of Forensic Identification* **2014**, *64* (2), 174-200.